A Data-Constrained Analysis of Joule Heating as a Solar Active Region Atmosphere Heating Mechanism over a 'Second' Sunspot Light Bridge

Brayden Sellers[1], Mehmet Sarp Yalim[2], Sanjiv K. Tiwari[3], Sushree Nayak[2], Christian Beck[4],
Debi Prasad Choudhary[5], Qiang Hu[2,6]

[1] The University of Alabama in Huntsville, Department of Atmospheric and Earth Science, Huntsville, AL, USA; [2] The University of Alabama in Huntsville, Center for Space Plasma and Aeronomic Research, Huntsville, AL, USA; [3] Bay Area Environmental Research Institute, Palo Alto, CA, USA; [4] National Solar Observatory, Boulder, CO, USA; [5] California State University, Northridge, Northridge, CA, USA; [6] The University of Alabama in Huntsville, Dept. of Space Science, Huntsville, AL, USA

Introduction

The coronal heating issue causes investigation of the heating mechanisms of the chromosphere and corona, in which temperatures increase multiple orders of magnitude over a few thousand kilometers above the photosphere. A proposed mechanism for the increase in thermal activity in the chromosphere is Cowling heating, namely the Joule heating due to dissipation of electric currents perpendicular to the magnetic field lines by Cowling resistivity. We plan to investigate the contribution of Cowling heating within the solar active region atmosphere corresponding to NOAA AR 12121 on 2014-07-27 from 14:02 to 17:58 UT(as a first analysis to investigate the presence of Cowling heating, we analyze at 14:12 UT), in particular over a sunspot light bridge (LB). Cowling heating has been observationally shown to heat an LB in Louis et al., 2021, Yalim et al., 2023. In this work, we analyze the Cowling heating as heating mechanism of a second sunspot LB towards the generalization of the results we obtained for the former.

Methods

The model used for calculating Cowling heating is defined by Yalim et al., 2020 in which the generalized Ohm's law relation takes multiple plasma parameters:

$Q = (\mathbf{E} + (\mathbf{B} \times \mathbf{v})) \cdot \mathbf{j} = \eta J_{\parallel}^2 + \boxed{\eta_c J_{\perp}^2}$ where η_c is the Cowling resistivity that is calculated from

$$\frac{\xi_n^2 B_0^2}{\alpha_n} = \eta_c - \eta$$

in which η is the Coulomb resistivity, ξ_n is the neutral fraction for a hydrogen plasma, B_0 is the magnetic field strength, and α_n is a factor expressed in terms of the effective collisional frequency of the plasma. According to our model, Cowling resistivity and thus Cowling heating (in dashed box) are dependent on plasma bulk density ϱ, temperature T, magnetic field $\boldsymbol{B}$, and electron and ion number densities n_e, n_i. These values, obtained from the solar atmosphere models, allow measurement of currents and heating mechanisms within a localized area of the active region.

Data

We observe a light bridge within NOAA AR12121 in Figure 2. We obtain the plasma parameters from tabulated data of semi-empirical Maltby M model (Maltby et al., 1986) that models sunspot umbrae, and magnetic field from the application of non-force-free field (NFFF) magnetic field extrapolation technique (Hu & Dasgupta, 2008) to SDO/HMI vector magnetogram data measured at 14:12 UT (see the dashed box in Figure 1, which corresponds to the AR 12121 in Figure 2).

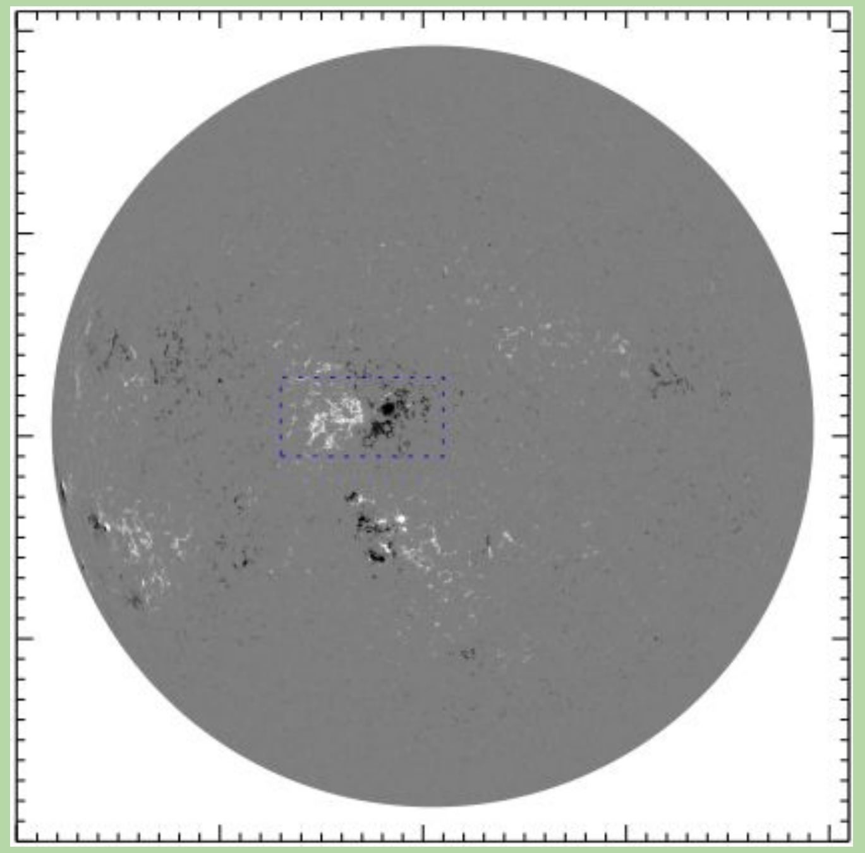

Figure 1 (left) SDO/HMI magnetogram measured on 2014-07-27 at 14:12 UT that shows NOAA AR 12121 in the dashed box; **Figure 2** (bottom) Field lines derived from the NFFF extrapolation overlaid on a composite image of the vertical component of the magnetic field and the SDO/AIA 171 Å image for the SHARP field of view (FOV) of AR 12121.

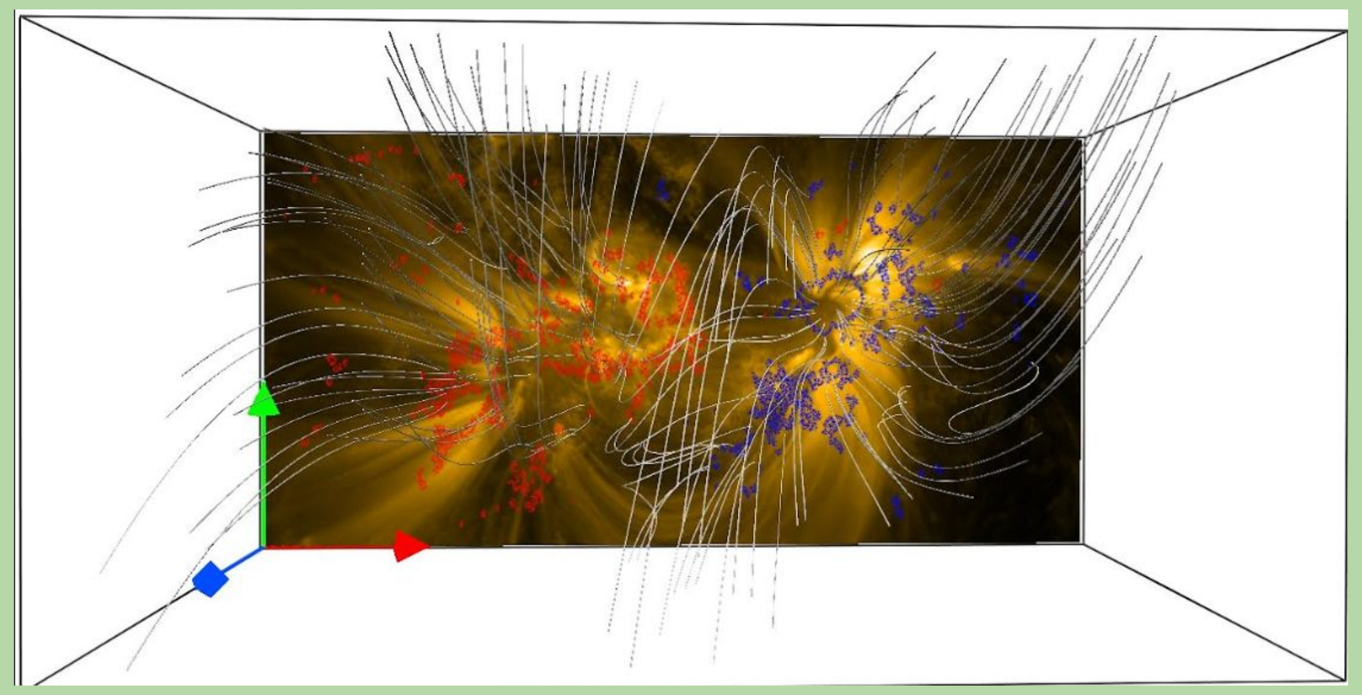

Results

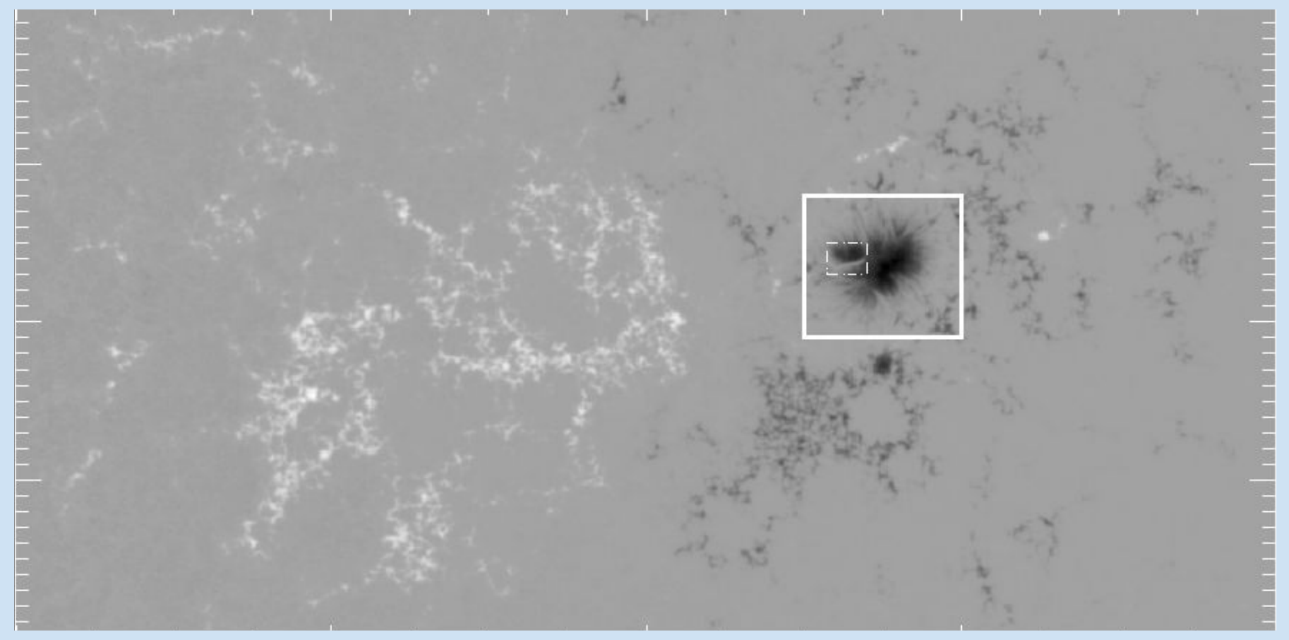

Figure 3. HMI Magnetogram of the region for which magnetic field lines were extrapolated: The large solid white box shows **Figure 4** in the context of the entire sunspot umbra, and the small dot-dashed box shows the LB studied.

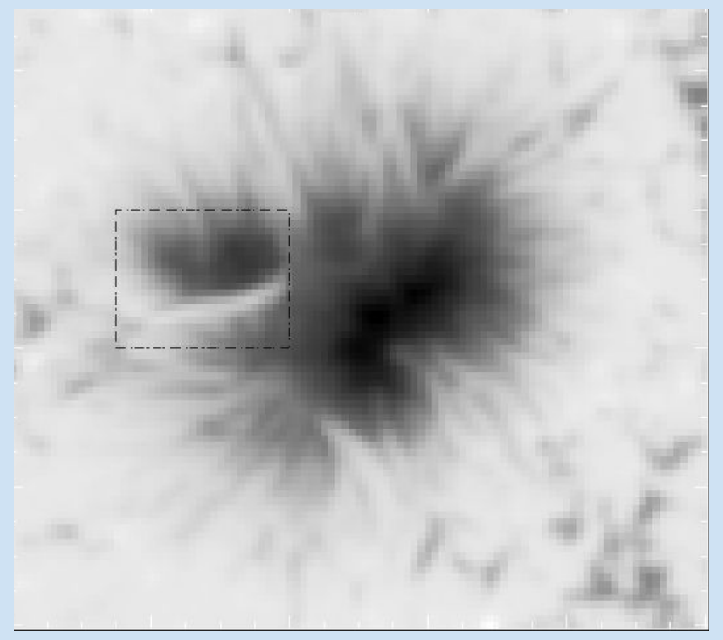

Figure 4. Region within solid white box in **Figure 3**: This image shows the entirety of the sunspot umbra and penumbra. The dot-dashed box shows the LB in the context of the sunspot.

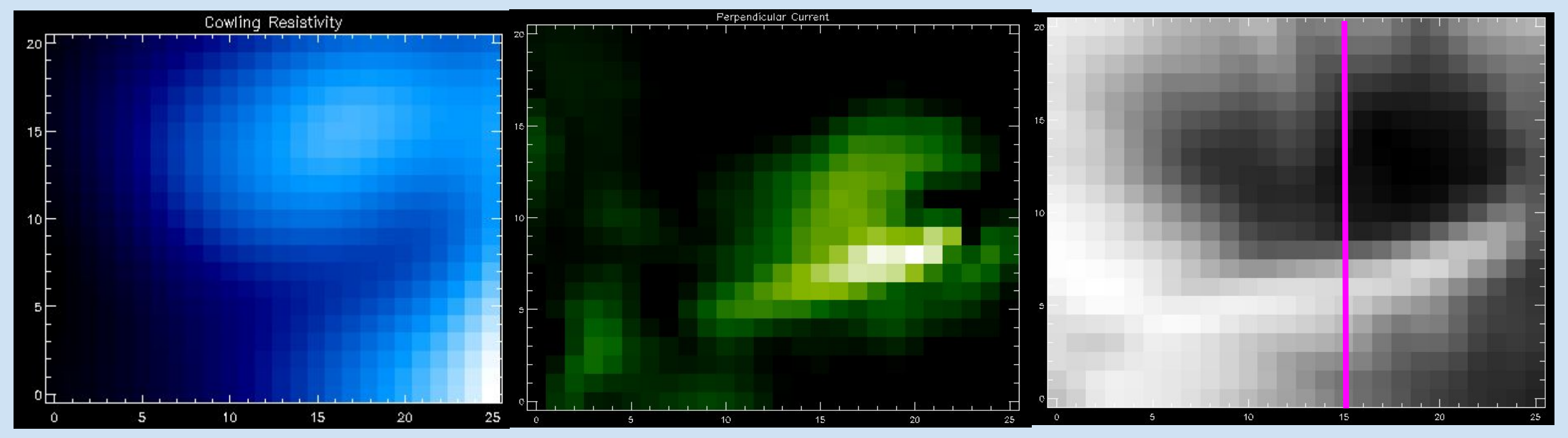

Figure 5 (left) shows the mean Cowling resistivity calculated by Maltby et al., 1986 within the LB region, while **Figure 6** (middle) shows the mean perpendicular current calculated using the same model. **Figure 7** (right) shows the position of the LB in the HMI Magnetogram data. We see that the most significant presence of perpendicular currents occurs localized within the LB.

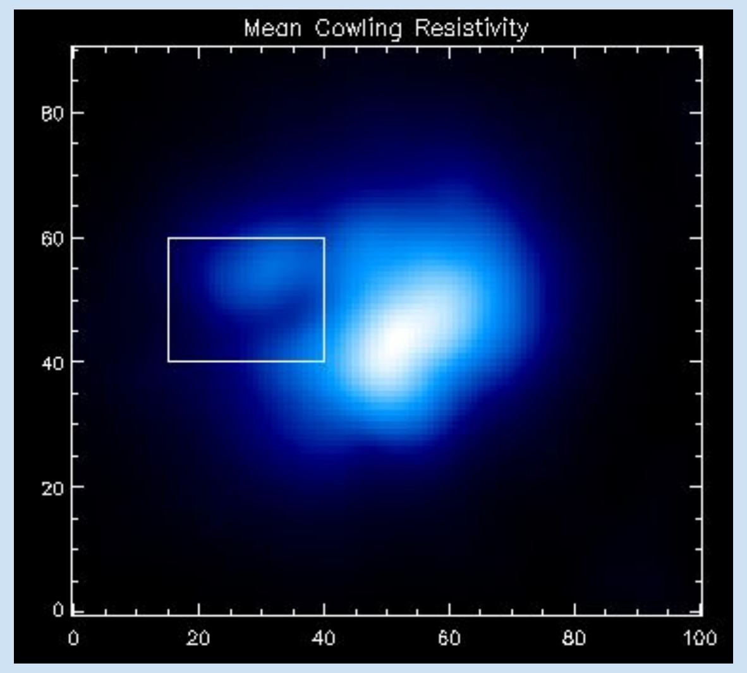

Figure 8. 2-Dimensional plot of the sunspot region, with the Cowling resistivity causing dissipation of perpendicular currents seen at its maximum in direct proximity to the LB within the region in **Figure 7**. Values are in [W/m^3] and averaged over height.

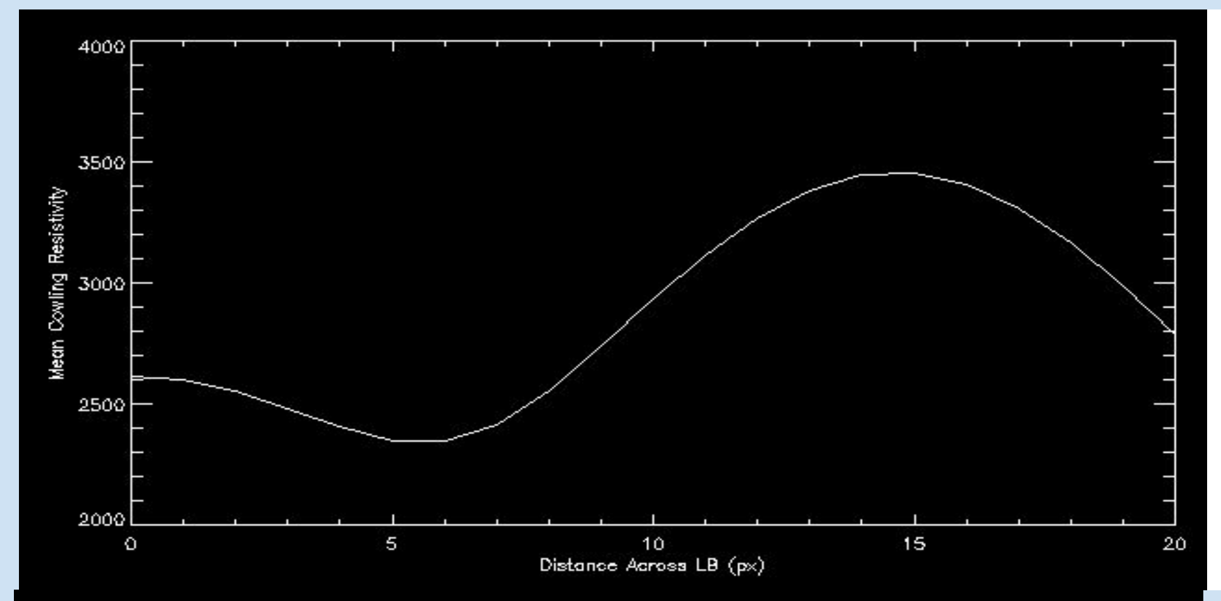

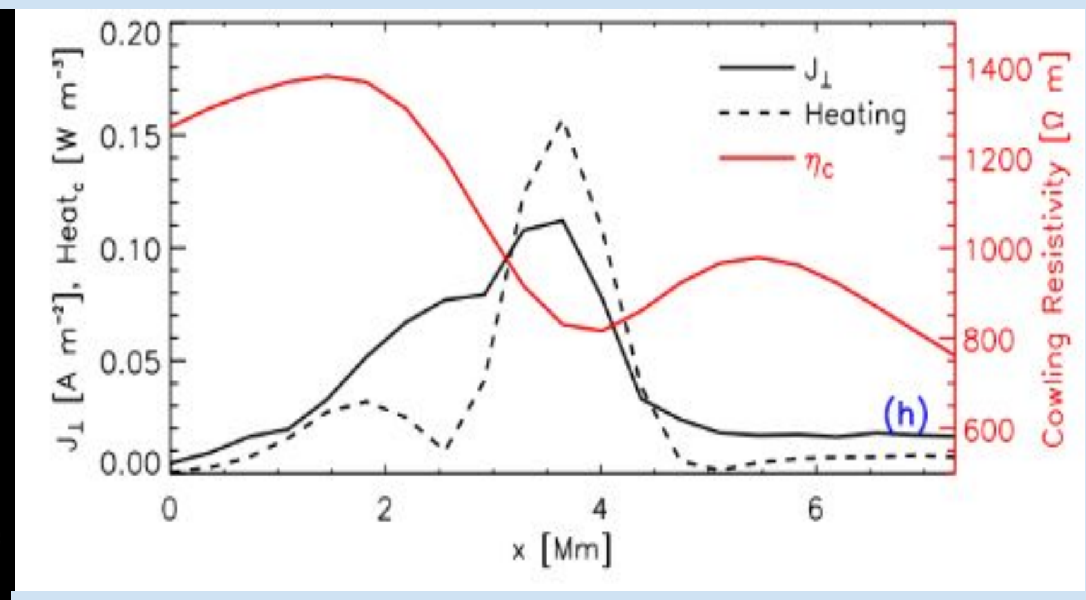

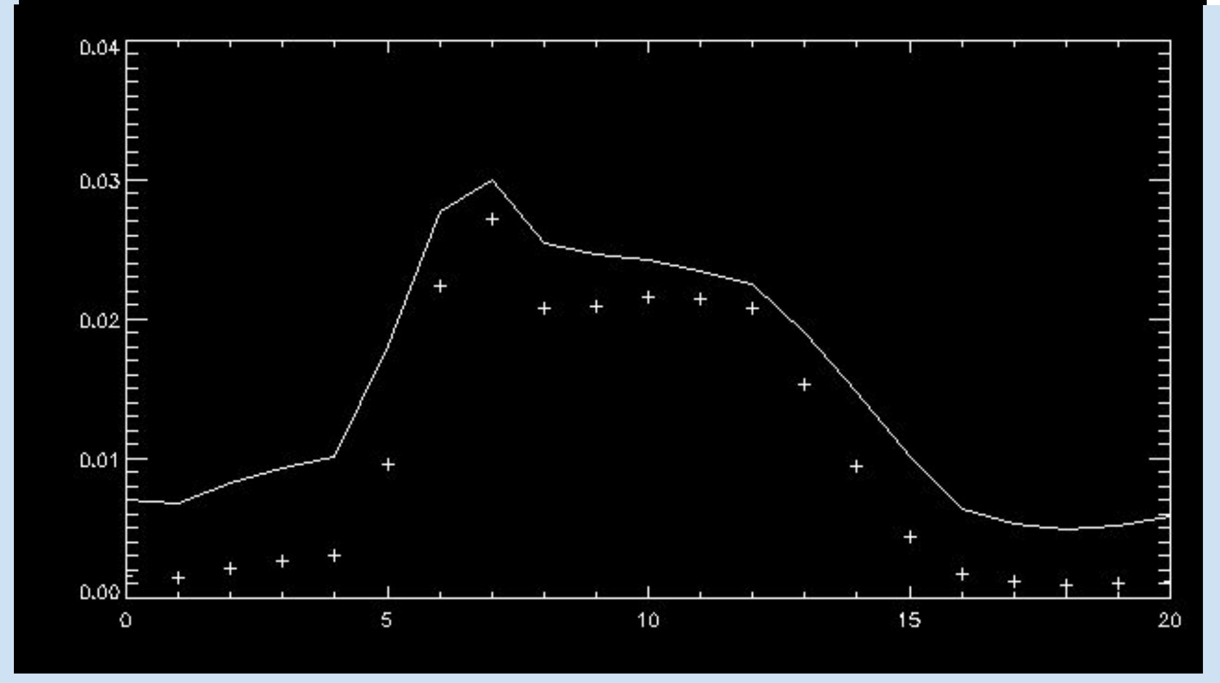

Figure 9 (top left) shows the mean Cowling resistivity across the vertical cut represented by the magenta line in **Figure 7**. **Figure 10** (top right) shows the calculations of the Maltby model run on the initial LB by Louis et al., 2021. **Figure 11** (bottom left) shows the mean Cowling heating (dotted line) across the cut identified in **Figure 10**. The solid line shows mean perpendicular current across the same cut.

Discussion, Conclusions, and Further Study

- The obtained values for Cowling resistivity, perpendicular currents, and the resulting Joule heating all show enhancement (a decrease in resistivity, and an increase in the other two parameters) in the LB with respect to its surroundings.
- Plots of the heating parameters across the LB show an increase/decrease to significant levels relative to the LB's surroundings. The visualization of perpendicular current, and Cowling resistivity on a vertical cut across the width of the LB (**Figures 9, 11)**) shows a substantial increase & decrease in their values, respectively compared to the region outside the LB, but still within the target AR.
- In the case of Cowling heating, the maximum observed values in the target region of **Figure 4** were found within the LB. This indicates, in addition to Louis et al., 2021, that Joule heating is a significant contributor to the overall heating of the LB atmosphere in a second LB which is an important step towards generalization of the results in the former. However, the two LBs still behave differently when it comes to the heating and its parameters due to the differences in magnetic field topology between the two LBs (see **Figures 9-11**).
- The nearly exclusive presence of perpendicular currents directly corresponding to the location of the LB indicates that the subsequent dissipation due to Cowling resistivity is more likely to occur in regions where LBs are prevalent: highly inclined magnetic fields with interactions between ions and neutrals.
- Considering the plasma parameter values discussed here come from tabulated solar atmosphere models (except for ***B***), constraining our model by observational temperature data will be an important next step. Observed spectral data from instruments like the Interface Region Imaging Spectrometer (IRIS) can be inverted to reveal 3-dimensional temperature data, so that fewer measurements of the chromospheric plasma parameters rely on tabulated model values.

References

Maltby, P., et al. 1986, ApJ, 306, 284
Louis, R. E., et al., 2021, A&A, 652, L4
Yalim, M. S., et al. 2023, J. Phys.: Conf. Series, 2544, 012006
Yalim, M. S., et al. 2020, ApJL, 899, L4
Hu, Q., & Dasgupta, B., 2008 Sol. Phys., 247, 87
Braginskii, S. I. 1965, Transport processes in a Plasma, in Reviews of Plasma Physics, Vol. 1 (New York: Consultants Bureau)

Acknowledgments

This work was supported by the NSF REU award AGS-1950831. MSY, SKT, SN, and DPC acknowledge partial support from NSF award AGS-2230633. Any opinions, findings, and conclusions or recommendations expressed in this material are those of the author(s) and do not necessarily reflect the views of the National Science Foundation. I would like to thank my mentor Dr. Sarp Yalim for his invaluable experience and knowledge, as well as my partner Dakota for his unwavering moral support throughout my research.